

Theoretical Model for Heterojunction Phototransistor in Optoelectronic Switch Configurations Part I: Optical Gain Characteristics

F. R. Tahir and R. S. Fyath
Department of Electrical Engineering, College of Engineering,
University of Basrah
Basrah – Iraq

Abstract

This paper presents a comprehensive analysis for the performance of heterojunction bipolar phototransistor (HPT) as an essential element for optoelectronic switch configurations. The theory of operation of the (HPT) is reviewed. Analytical expressions are derived for transistor current components, optical gain G_{opt} , and DC current gain in common – emitter configuration h_{FE} . The analysis enables one to study the influence of various structure parameters and incident optical power on the optical gain characteristics of the (HPT). Simulation results are presented for a $1.3 \mu m$ $In_{0.53} Ga_{0.47} As/InP$ structure.

نموذج نظري للترانزستور الضوئي ذو المفروق المتباين المستخدم
في تراكيب المفتاح الضوئي – الإلكتروني
جزء I : مميزات الكسب الضوئي

فاضل رحمه طاهر و رعد سامي قياض
قسم الهندسة الكهربائية، كلية الهندسة،
جامعة البصرة
البصرة – العراق

الخلاصة:

هذا البحث يقدم تحليل شامل لأداء الترانزستور الضوئي ذو المفروق المتباين (HPT) كعنصر أساس في تراكيب المفتاح الضوئي – الإلكتروني. تم عرض مبدأ العمل لـ (HPT) واشتقاق التعابير الخاصة بمركبات التيار، الكسب الضوئي G_{opt} ، وكسب التيار لربط الباعث المشترك h_{FE} . التحليل النظري المقدم يمكن من دراسة تأثير مختلف بارامترات البنية والقدرة الساقطة على مميزات الكسب الضوئي لهذا الترانزستور. قدمت نتائج المحاكاة قُدمت للتراكيب $In_{0.53} Ga_{0.47} As/ InP$ ويعمل بطول موجي $1.3 \mu m$.

1. Introduction

The heterojunction bipolar phototransistors (HPTs) have attracted a great deal of interest as an alternative to avalanche photodetectors. The HPTs can provide large optical gain without excess noise that characterizes avalanche photodetectors [1]. Furthermore, HPTs have proven to be suitable for vertical integration with other components [2]. The integration of HPTs and vertical cavity surface-emitting lasers (VCSELs) represents a promising two-dimensional approach to high-throughput optical data processing and optical switching networks [3, 4].

The potential advantages of heterojunction transistors include [5-8];

- i. Higher emitter efficiency, since holes (in N- p- n structure) following from base to emitter are blocked by the higher barrier in the valence band.
- ii. Decreased base resistance, since the base can be heavily doped without sacrificing emitter efficiency.
- iii. Decrease emitter current crowding because of a low voltage along the emitter junction.
- iv. Improved frequency response because of higher current gain and a lower base resistance.
- v. The quantum efficiency in the heterojunction photodetector does not critically depend on the distance of junction from the surface, because a large-bandgap material can be used as a window for the transmission of optical power.
- vi. The heterojunction can provide unique material combinations so that the

quantum efficiency and speed of response can be optimized for a given optical wavelength.

In this paper, the basic physical structure and the theory of operation of HPT will be discussed to identify the main parameters affecting its operation as an optoelectronic switch. The basic idea behind the operation of HPT is briefly described in Section 2. In Section 3, the current relationships in the emitter, base, and collector are calculated by solving the diffusion equation. Section 4 shows the dependence of optical gain on the current gain parameter h_{FE} associated with common-emitter configuration (CEC), and Kroemer's factor γ_0 . The simulation results, are presented in Section 5. The main findings of the study are given Section 6.

2. Principles of Operation of HPT

The basic structure of HPT and the corresponding energy band are shown in Figs. (1a) and (1b), respectively. The HPT differs from a conventional heterojunction bipolar transistor by having a large collector junction as the light-collecting element and without any external connection to the base (floating base). The device is in the form of emitter-up configuration. The power incidents on the device will pass through the wide-gap emitter unattenuated and is absorbed in subsequent base, and base-collector depletion regions. The absorbed light generates electron-hole pair in the two layers, and the electrons that generated in base layer move towards the collector region. The photogenerated holes are swept into the base and are accumulated

there due to a large potential barrier in the valence band at heterointerface of emitter junction. This leads to increase the forward bias of emitter junction which causes a large electron current to flow from the emitter to the collector. A significant amount of photocurrent gain, to maintain the charge – neutrality condition in the base, can be achieved by this process [8].

3. Current Equations in HPT

This section is devoted to derive the main equations describing the current components in the HPT. The analysis is carried out under the following assumptions; (i) The illumination is uniformly incident over the frontal area of the emitter layer in a direction perpendicular to the junction planes. (ii) The HPT is biased in a floating base condition, and (iii) The emitter junction is forward biased ($V_e > 0$), while collector junction reverse biased ($V_c < 0$), as shown in Fig. (1b). The electron and hole currents due to the diffusion of carries will be calculated in the presence of light for the emitter, base, and collector regions, respectively.

3.1 Emitter Region

In the emitter layer, the distribution of excess holes ($P_e(x) - p_{e0}$) in the steady states condition can be obtained by solving the continuity equation [5].

$$D_e \frac{d^2(P_e - p_{e0})}{dx^2} - \frac{P_e - p_{e0}}{\tau_e} + U_e \exp(-\alpha_e x) = 0 \quad \dots(1)$$

where the subscript e is used to denote the emitter. Further

D_e = Diffusion constant of minority carriers.

τ_e = Life time of minority carriers.

p_{e0} = Equilibrium hole concentration in the emitter.

α_e = Absorption constant of light.

In eqn.1, U_e is the generation rate of holes caused by incident power and it is equal to [5]:

$$U_e = \alpha_e \eta_e \Phi_0 \quad \dots(2)$$

where η_e is the quantum efficiency in the emitter, and Φ_0 is the incident light flux at the emitter surface. The second term of eqn. 1 represents the recombination rate of carriers in the emitter region.

The boundary conditions for the emitter layer are [5]

$$D_e \frac{d(P_e - p_{e0})}{dx} = S_e (P_e - p_{e0}) \quad \text{at } x = 0 \quad \dots(3a)$$

$$(P_e - p_{e0}) = p_{e0} (\exp(V_e / V_T) - 1) \quad \text{at } x = W_e \quad \dots(3b)$$

where V_e is the emitter junction voltage, V_T is the voltage – equivalent of temperature, W_e is thickness of emitter, S_e is the surface recombination velocity at the emitter surface.

The hole current flowing into emitter junction is computed from [5],

$$I_{pe} = qAD_e \left. \frac{d(P_e - p_{e0})}{dx} \right|_{x=W_e} \quad \dots(4)$$

where q is the electron charge, and A is the cross section- area of the transistor.

Using eqns. 1- 4 yields:

$$I_{pe} = I_{pi} [\exp(V_e / V_T) - 1] - I_{m1} F_1 \quad \dots(5)$$

where

$$I_{m1} = qA \frac{D_e}{L_e} \left(\left(\alpha_e L_e + \frac{H_2}{H_1} \right) \exp(-\alpha_e W_e) - \frac{1}{H_1} \left(\frac{S_e L_e}{D_e} + \alpha_e L_e \right) \right) \quad \dots(6a)$$

$$I_{pi} = qA \frac{D_e}{L_e} \frac{H2}{H1} p_{e0} \quad \dots(6b)$$

and

$$H1 = \frac{S_e L_e}{D_e} \sinh\left(\frac{W_e}{L_e}\right) + \cosh\left(\frac{W_e}{L_e}\right) \quad \dots(7a)$$

$$H2 = \sinh\left(\frac{W_e}{L_e}\right) + \frac{S_e L_e}{D_e} \cosh\left(\frac{W_e}{L_e}\right) \quad \dots(7b)$$

$$F1 = \frac{L_e^2 U_e}{D_e (1 - \alpha_e^2 L_e^2)} \quad \dots(7c)$$

Here, L_e is the diffusion length of the minority carriers in the emitter.

3.2 Base Region

In the neutral base region the diffusion equation for the electrons reads [5]

$$D_b \frac{d^2(N_b - n_{b0})}{dx^2} - \frac{(N_b - n_{b0})}{\tau_b} + U_b \exp(-\alpha_b x) = 0 \quad \dots(8)$$

where

$$U_b = \alpha_b \eta_b \Phi_o \exp(-\alpha_e W_e) \quad \dots(9)$$

The boundary conditions in the base layer are

$$(N_b - n_{b0}) = n_{b0} (\exp(V_e / V_T) - 1) \quad \text{at } x = W_e \quad \dots(10a)$$

$$(N_b - n_{b0}) = n_{b0} (\exp(V_e / V_T) - 1) \quad \text{at } x = W_e + W_b \quad \dots(10b)$$

where V_e is the reverse bias of the collector junction voltage.

The electron current following into the emitter junction I_{nbe} computed from [5].

$$I_{nbe} = qA D_b \frac{d(N_b - n_{b0})}{dx} \Big|_{x=W_e} \quad \dots(11)$$

Using eqns. 8-11 yields:

$$I_{nbe} = qA \frac{D_b}{L_b \sinh\left(\frac{W_b}{L_b}\right)} \left((n_{b0} (\exp(V_e / V_T) - 1) - \right.$$

$$n_{b0} (\exp(V_e / V_T) - 1) \cosh\left(\frac{W_b}{L_b}\right) +$$

$$F3 \left(\cosh\left(\frac{W_b}{L_b}\right) - \exp(-\alpha_b W_b) -$$

$$\left. \alpha_b L_b \sinh\left(\frac{W_b}{L_b}\right) \right) \quad \dots(12)$$

where

$$F3 = \frac{L_b^2 U_b}{D_b (1 - \alpha_b^2 L_b^2)} \quad \dots(13)$$

All the symbols in eqns. 8-13 have their usual meanings. Notice that the subscript b is used to describe the parameters in the base region.

Following the same approach, the electron current flowing into the collector junction is calculated from [5]

$$I_{nbc} = qA D_b \frac{d(N_b - n_{b0})}{dx} \Big|_{x=W_e + W_b} \quad \dots(14)$$

$$I_{nbc} = qA \frac{D_b}{L_b \sinh\left(\frac{W_b}{L_b}\right)} \left(n_{b0} (\exp(V_e / V_T) - 1) \right.$$

$$\cosh\left(\frac{W_b}{L_b}\right) - n_{b0} (\exp(V_e / V_T) - 1) \sinh\left(\frac{W_b}{L_b}\right) +$$

$$F3 \left((1 - \exp(-\alpha_b W_b)) \cosh\left(\frac{W_b}{L_b}\right) \right.$$

$$\left. \left. + \alpha_b L_b \sinh\left(\frac{W_b}{L_b}\right) \right) \right) \quad \dots(15)$$

3.3 Collector Region

In the collector region the diffusion equation for holes reads [5]

$$D_c \frac{d^2(P_c - p_{co})}{dx^2} - \frac{(P_c - p_{co})}{\tau_c} + \dots (16)$$

$$U_c \exp(-\alpha_c(x - W_e)) = 0$$

where the subscript c denotes the collector region and [5]

$$U_c = \eta_c \alpha_c \Phi_o \exp(-(\alpha_c W_e + \alpha_b W_b)) \dots (17)$$

There are two boundary conditions to be satisfied here. At the collector surface we have, surface recombination with recombination velocity S_c

$$D_c \frac{d(P_c - p_{co})}{dx} = -S_c(P_c - p_{co}) \dots (18a)$$

at $x = W_e + W_b + W_c$

Eqn.18a states that back surface recombination takes place at the collector surface.

At the depletion edge $x = W_e + W_b + W_D$, the excess carrier density is

$$P_c - p_{co} = p_{co}(\exp(V_c / V_T) - 1) \dots (18b)$$

at $x = W_e + W_b + W_D$

where W_D is the depletion region of base - collector region.

The hole current flowing into collector junction is computed from

$$I_{pc} = qAD_c \frac{d(P_c - p_{co})}{dx} \Big|_{x=W_e+W_b+W_D} \dots (19)$$

Using eqns. 16- 19 yields:

$$I_{pc} = qA \frac{D_c}{L_c} \left(F4 \left[\frac{E2}{E1} - \alpha_c L_c + \frac{1}{E1} \left(\alpha_c L_c - \frac{S_c L_c}{D_c} \right) \exp(\alpha_c(W_c - W_D)) \right] - \frac{E2}{E1} p_{co} (\exp(V_c / V_T) - 1) \right) \dots (20)$$

where

$$E1 = \sinh\left(\frac{W_c - W_D}{L_c}\right) + \dots (21a)$$

$$\frac{S_c L_c}{D_c} \cosh\left(\frac{W_c - W_D}{L_c}\right)$$

$$E2 = \cosh\left(\frac{W_c - W_D}{L_c}\right) + \dots (21b)$$

$$\frac{S_c L_c}{D_c} \sinh\left(\frac{W_c - W_D}{L_c}\right)$$

$$F4 = \frac{L_c^2 U_c}{D_c (1 - \alpha_c^2 L_c^2)} \dots (21c)$$

Eqn. 20 can be simplified for the special case when $W_c \gg L_c \gg W_D$

$$I_{pc} = qA \frac{D_c}{L_c} (F4(1 - \alpha_c L_c) - p_{co} (\exp(V_c / V_T) - 1)) \dots (22)$$

4. Optical Gain G_{opt}

In this section, the optical gain of a HPT is calculated using transistor current equations given in the previous section. The DC current gain h_{FE} in the common - emitter - configuration (CEC) is also calculated, and the relation between G_{opt} and h_{FE} is obtained.

4.1 Expression of G_{opt}

The total current I_T is constant through the device and hence [see Fig. 1b].

$$I_T = I_{pc} - I_{nbc} = I_{pe} - I_{nbc} \dots (23)$$

Using the expression of I_{pc} and I_{nbc} derived in section 3, the following expression can be obtained for I_T

$$I_T = I_{yt} \left((\exp(V_c / V_T) - 1) + \cosh\left(\frac{W_b}{L_b}\right) \right) + \Phi_o (y_3 - y_2) - I_{pco} \dots (24)$$

$$I_{y1} = qA \frac{D_b n_{bo}}{L_b \sinh\left(\frac{W_b}{L_b}\right)} \quad \dots(25a)$$

$$y_2 = qA \frac{L_b \alpha_b \eta_b \exp(-\alpha_e W_e)}{(1 - \alpha_b^2 L_b^2) \sinh\left(\frac{W_b}{L_b}\right)} + \left(1 - \exp(\alpha_b W_b) \cosh\left(\frac{W_b}{L_b}\right) + (\alpha_b L_b) \sinh\left(\frac{W_b}{L_b}\right)\right) \quad \dots(25b)$$

$$y_3 = qA \frac{D_e}{L_e} F_4 (1 - \alpha_e L_e) \quad \dots(25c)$$

$$I_{pco} = qA \frac{D_e}{L_e} p_{\infty} (\exp(V_e / V_T) - 1) \quad \dots(25d)$$

The increase of I_T due to Φ_o can be evaluated from eqn. 24 as follows

$$\Delta I_T = I_{y1} \Delta \left[e^{V_e / V_T} \right] + (y_3 - y_2) \Phi_o \quad \dots(26)$$

where $\Delta[\exp(V_e / V_T)]$ is related to the increase of the forward bias at the emitter junction due to the presence of Φ_o , and can be evaluated from eqn. 24.

$$\Delta[\exp(V_e / V_T)] = \frac{\Phi_o (y_2 - y_3 - I_{m2} F_1 - y_4)}{I_{y1} \left(\cosh\left(\frac{wb}{L_e}\right) - I_{p1} \right)} \quad \dots(27)$$

where;

$$y_4 = qA \frac{U_b}{\Phi_o L_b \sinh\left(\frac{wb}{L_b}\right)} \left(\cosh\left(\frac{we}{L_b}\right) - \exp(-\alpha_b W_b) - (\alpha_b L_b) \sinh\left(\frac{W_e}{L_b}\right) \right) \quad \dots(28)$$

The optical gain is defined as $\Delta I_T / qA \Phi_o$ and can be calculated using eqns. 26- 28.

$$G_{opt} = \frac{I}{qA} \frac{\gamma \left((y_2 - y_3) \left(\cosh\left(\frac{W_b}{L_b}\right) - 1 \right) - I_{m1} F_1 / \Phi_o - y_4 \right)}{\left(\gamma \left(1 - \cosh\left(\frac{W_b}{L_b}\right) \right) - 1 \right)} \quad \dots(29)$$

where;

$$\gamma = \gamma_o \frac{H_1}{H_2 \sinh\left(\frac{W_b}{L_b}\right)} \quad \dots(30a)$$

Notice that G_{opt} is independent on received optical power which is an expected result since no saturation effects are included in the analysis. The factor γ_o originally derived by Kroemer, is the ratio of injected electron to injected hole current at the emitter - base heterojunction. It depends on the minority carriers diffusivity, diffusion length, minority carriers density, and conduction - and valence - band densities of states (N_c and N_v) in the emitter and base as well as ΔE_g , and is given by [7].

$$\gamma_o = \left(\frac{D_b L_e N_{De}}{D_e L_b N_{Ah}} \right) \left(\frac{N_{cb} N_{vb}}{N_{ce} N_{ve}} \right) \exp\left(\frac{\Delta E_g}{KT}\right) \quad \dots(30b)$$

where N_{De} is the donor concentration in emitter, N_{Ah} is the acceptor concentration in the base, and $\Delta E_g = E_{gc} - E_{gb}$, where E_{gc} (E_{gb}) is the bandgap energy for the emitter (base).

4. 2. The Relation between G_{opt} and I_{EE}

The current gain α for a common - base configuration in the absence of illumination can be computed by setting $\Phi_o = 0$ in eqn. 5. The terminal current through

the emitter junction is given by

$$I = (I_{nbe} - I_{pe})|_{\Phi_s=0}$$

The parameter α is computed from

$$\alpha = \gamma_b \gamma_e \quad \dots (31)$$
 where γ_e is the emitter junction efficiency,
 and γ_b the base transport factor [6].

$$\gamma_b = \frac{I_{nbc}}{I_{nbc}}$$

$$= \frac{\left(\cosh\left(\frac{W_e}{L_b}\right) + (\exp(V_e / V_T) - 1) \right)}{\left(1 + \cosh\left(\frac{W_b}{L_b}\right) (\exp(V_e / V_T) - 1) \right)} \quad \dots(32)$$

$$\gamma_e = \frac{I_{nbc}}{I_e}$$

$$= \frac{I_{y1} \left(1 + \cosh\left(\frac{W_e}{L_b}\right) (\exp(V_e / V_T) - 1) \right)}{\left((\exp(V_e / V_T) - 1) (I_{p1} + I_{y1} \cosh\left(\frac{W_b}{L_b}\right)) + I_{y1} \right)} \quad \dots(33)$$

For a common – emitter configuration [6]

$$h_{FE} = \frac{\gamma_b \gamma_e}{1 - \gamma_b \gamma_e} \quad \dots(34)$$

Using the expression of γ_e and γ_b given above and assuming $V_e \gg V_T$, one can arrive to the following expression to describe h_{FE} .

$$h_{FE} = \frac{\gamma_o \left(\frac{H1}{H2} \right) \left(\frac{1}{\sinh\left(\frac{W_b}{L_b}\right)} \right)}{1 + \gamma_o \left(\frac{H1}{H2} \right) \frac{(\cosh\left(\frac{W_b}{L_b}\right) - 1)}{\sinh\left(\frac{W_b}{L_b}\right)}} \quad \dots(35)$$

Using eqn. 29 and eqn. 35, one can get:

$$G_{opt} = \frac{h_{FE}}{qA} \left((y_1 - y_2) \left(\cosh\left(\frac{W_b}{L_b}\right) - 1 \right) + I_{nbc} (1 + \gamma_e) \right) + \frac{h_{FE} (y_1 - y_2)}{qA \gamma} \quad \dots(36)$$

It is interesting to examine eqn. 35 for the following special cases

i.) if $\gamma_o \ll \frac{\sinh\left(\frac{W_b}{L_b}\right)}{\frac{H1}{H2} (\cosh\left(\frac{W_b}{L_b}\right) - 1)}$... (37a)

then eqn. 35 becomes

$$h_{FE} = \gamma \quad \dots(37b)$$

ii.) if $\gamma_o \gg \frac{\sinh\left(\frac{W_b}{L_b}\right)}{\frac{H1}{H2} (\cosh\left(\frac{W_b}{L_b}\right) - 1)}$... (38a)

$$h_{FE} = \frac{1}{\left(\cosh\left(\frac{W_b}{L_b}\right) - 1 \right)} \quad \dots(38b)$$

5. Simulation Results

Simulation results are presented for a 1.3 μm $\text{In}_{0.53}\text{Ga}_{0.47}\text{As}/\text{InP}$ HPT using the parameter values listed in Table I.

Figure 2 shows the dependence of h_{FE} on base width W_b for three different values of the minority carriers diffusion length $L_b = 0.8, 1.6$ and $2.4 \mu\text{m}$. h_{FE} greater than 1000 may be obtained by controlling the values of base width and the doping concentration in the base.

Figures 3 and 4 depict, respectively, the variation of h_{FE} and optical gain G_{opt} on Kroemer's factor γ_o for two values of base width, $W_b = 90 \text{ nm}$ and 50 nm . Notice that both h_{FE} and G_{opt} are increasing functions of γ_o , and they increase when the base width reduces. However, increasing γ_o beyond 1000 (100) has almost a negligible effect on h_{FE} and G_{opt} when $W_b = 50 \text{ nm}$ (90 nm). Notice further

that reducing W_b from 90 nm to 50 nm will enhance h_{FE} (and hence G_{opt}) by approximately 4 times when $\gamma_o \gg 100$.

6. Conclusion

Analytical expressions for current components have been derived for a heterojunction phototransistor (HPT). Optical gain G_{opt} and DC current gain h_{FE} under various operating conditions. Simulation results presented for a 1.3 μm InGaAs/InP HPT reveal that h_{FE} greater than 1000 can be obtained. Further, reducing the base width from 90 nm to 50 nm will enhance both h_{FE} and G_{opt} by approximately four times when the Kroemer factor $\gamma_o \gg 100$.

Table-1 Parameters for the $\text{In}_{0.53}\text{Ga}_{0.47}\text{As} - \text{InP}$ used in the simulation.

| Emitter | Base | Collector |
|-----------------------------------|---|--------------------------------------|
| $E_{eg} = 1.35 \text{ eV}$ | $E_{gb} = 0.75 \text{ eV}$ | $E_{gc} = 0.75 \text{ eV}$ |
| $D_e = 5.6 \text{ cm}^2/\text{s}$ | $D_b = 300 \text{ cm}^2/\text{s}$ | $N_{Dc} = 10^{16} \text{ cm}^{-3}$ |
| $ND_e = 10^{15} \text{ cm}^{-3}$ | $N_{Ab} = 2 \times 10^{18} \text{ cm}^{-3}$ | $W_c = 3 \mu\text{m}$ |
| $m_e^* = 0.08 m_0$ | $W_b = 0.05 \mu\text{m}$ | $L_c = 1.1 \mu\text{m}$ |
| $m_e^* = 0.64 m_0$ | $L_b = 0.9 \mu\text{m}$ | $n_{ic} = 10^{11} \text{ cm}^{-3}$ |
| $\epsilon_{re} = 12.4$ | $m_{cb}^* = 0.4 m_0$ | $v_s = 10^7 \text{ cm/s}$ |
| | $m_{cb}^* = 0.44 m_0$ | $\alpha_c = 10^{-6} \text{ cm}^{-1}$ |
| | $\alpha_b = 10^4 \text{ cm}^{-1}$ | |
| | $n_{ip} = 10^{11} \text{ cm}^{-3}$ | |
| | $A = 5 \times 10 \mu\text{m}^2$ | |
| | $c_e = 24 \text{ fF}$ | |
| | $c_c = 450 \text{ fF}$ | |
| | $\eta = 0.7$ | |
| | $V_T = KT/q = 26 \text{ mV}$ | |

Notes:

- n_i = Intrinsic concentration.
- ϵ_r = Relative dielectric constant.
- m_0 = Free – electron mass.

References

- [1] O. Sjölund and A. Larsson, "Uniform Array of Resonant Cavity Enhanced InGaAs- AlGaAs Heterojunction Phototransistors," IEEE Photon. Technol. Lett. Vol. 7, pp. 682- 684, (1995).
- [2] B. Lu, P. Zhou, Y. – Chen Lu, and J. Cheng, "Reconfigurable Binary Optical Routing Switches with Fan-Out Based on the Integration of GaAs/ AlGaAs Surface – Emitting Lasers and Heterojunction Phototransistors," IEEE Photon. Technol. Lett. 6, 222- 225 (1994).
- [3] B. Lu, P. Zhou, Y. – C. Lu, and J. Cheng, "Binary Optical Switch and Programmable Optical Logic Gate Based on the Integration of GaAs/ AlGaAs Surface – Emitting Lasers and Heterojunction Phototransistors," IEEE Photon. Technol. Lett. 6, 398- 401 (1994).
- [4] S. M. Sze, "Devices Semiconductor Physics and Technology" Marry Hill, New Jersey 1985.
- [5] J. Cheng and P. Zhou, "Integrable Surface- Emitting Laser- Based Optical Switches and Logic Gates for parallel Digital Optical Computing", Appl. Opt. Lett. 31, 5592- 5602 (1992).
- [6] J. C. Campbell, and K. Ogawa, "Heterojunction Phototransistor for Long- Wavelength Optical Receivers", J. Appl. Phys. 53, 1203- 1208 (1982).
- [7] J. C. Campbell and A. G. Deytal, "Avalanche InP/InGaAs Heterojunction Phototransistor", IEEE J. Quantum Electron. QE- 19, 1134- 1137 (1983).
- [8] B. C. Roy, and N. B. Chakrabarti, "Gain and Frequency Response of a Graded- Base Heterojunction Bipolar Phototransistor", IEEE Trans. Electron Devices, ED- 7. 1482- 1490 (1987).

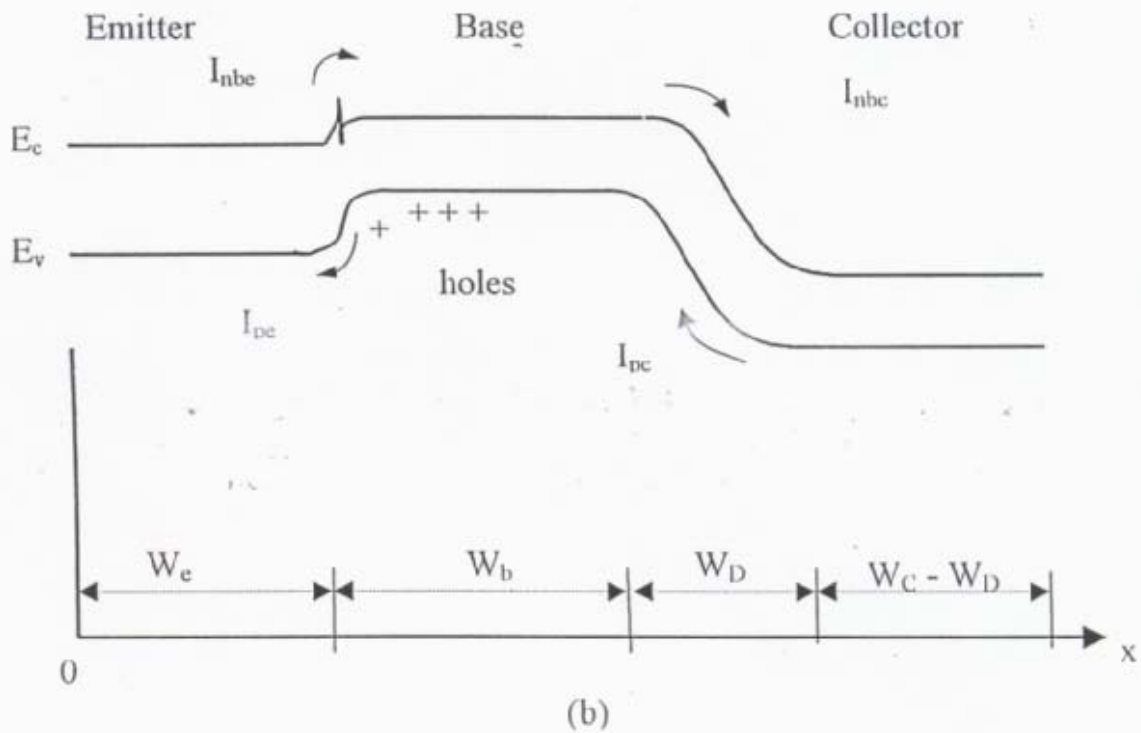
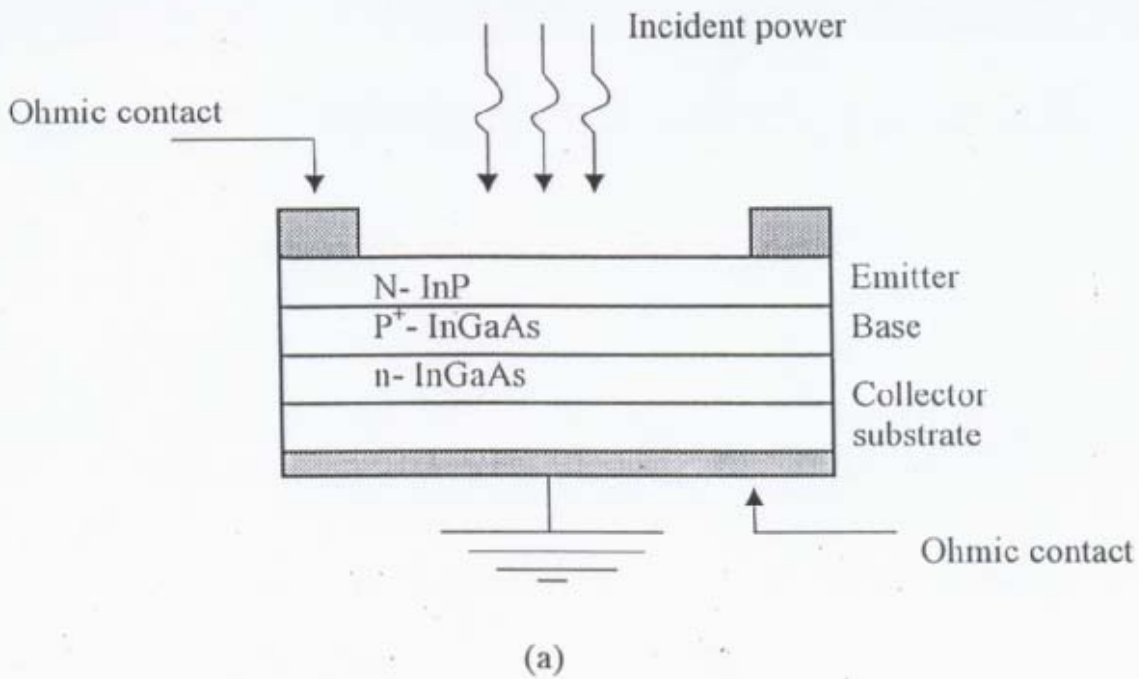


Fig.1 Heterojunction phototransistor HPT. (a) Physical structure and (b) Energy-Band diagram, and current components.

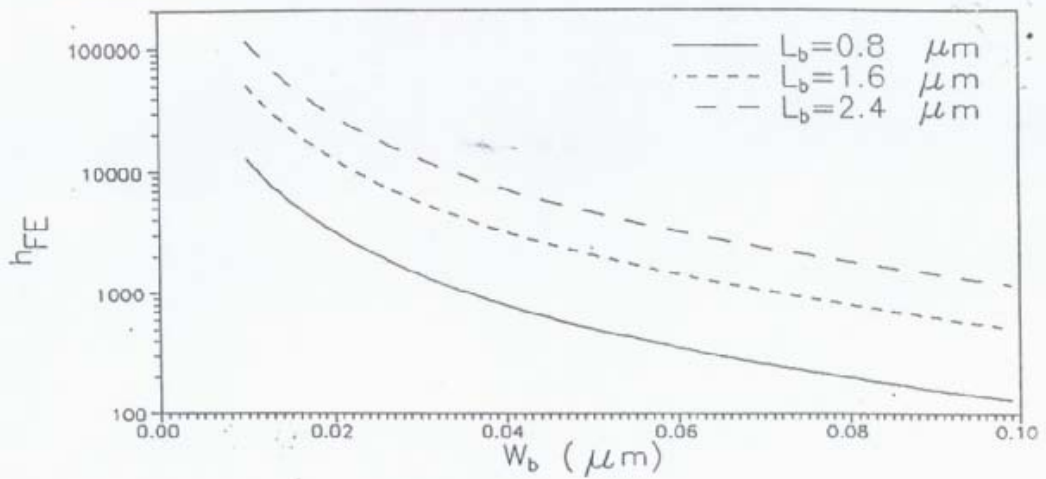


Fig. (2)- DC current gain h_{FE} versus base width W_b and taking L_b as an independent parameter.

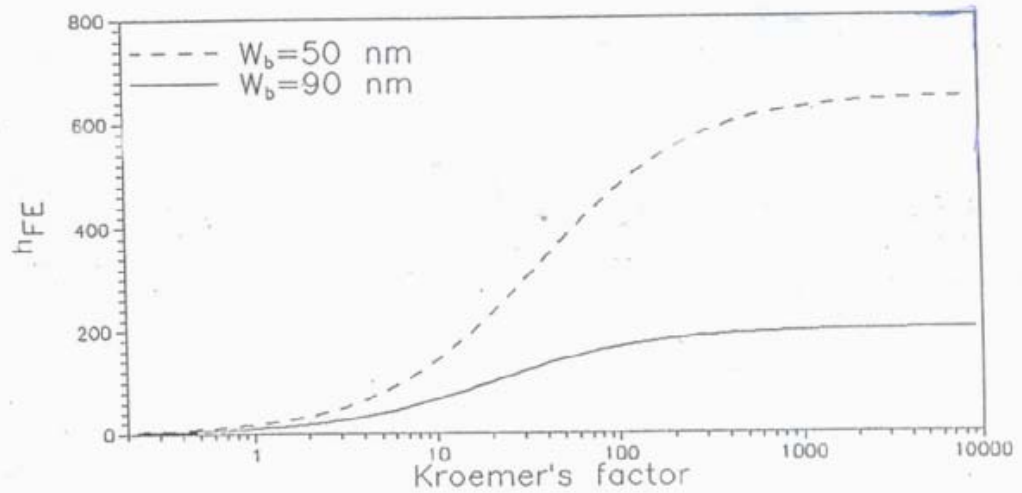


Fig. (3)- DC current gain h_{FE} as a function of Kroemer's factor and taking W_b as an independent parameter.